Implications of memory CD8 T cell quality for protective immunity

Redeker, A.

CHAPTER 5

Viral inoculum dose impacts memory T-cell inflation

Anke Redeker, Suzanne P.M. Welten
and Ramon Arens

European Journal of Immunology 2014 Apr;44(4):1046-5

5

ABSTRACT

Memory T cell inflation develops during certain persistent viral infections and is characterized by the accumulation and maintenance of large numbers of effector-memory T cell populations, albeit with varying degrees in size and phenotype among infected hosts. The underlying mechanisms that control the generation of memory T cell inflation are not yet fully understood. Here, we dissected CMV-specific memory T cell formation and its connection to the initial infectious dose by varying the inoculum size. After low dose inoculum with mouse CMV, the accumulation of inflationary memory T cells was severely hampered and correlated with reduced reservoirs of latent virus in non-hematopoietic cells and diminished antigen-driven T cell proliferation. Moreover, lowering of the initial viral dose turned the characteristic effector memory-like inflationary T cells into more central memory-like cells as evidenced by the cell-surface phenotype of $CD27^{high}$, $CD62L^{+}$, $CD127^{+}$ and $KLRG1^{-}$, and by improved secondary expansion potential. These data show the impact of the viral inoculum on the degree of memory T cell inflation and provide a rationale for the observed variation of human CMV-specific T cell responses in terms of magnitude and phenotype.

INTRODUCTION

Memory T cell inflation arises during certain persistent viral infections and is characterized by the accumulation and maintenance of large numbers of effector-memory T cell populations (1). It is especially prominent during the course of cytomegalovirus (CMV) infection and observed in different species including humans, monkeys, and mice (2-5). Studies in experimental models of CMV infection imply that memory T cell inflation is driven by repetitive antigen exposure likely due to sporadic viral re-activation (6-10). The characteristic effector-like phenotype of the inflationary memory $CD8^+$ T cells (i.e. $CD27^{low}$, $CD28^-$, $CD62L^-$, $CD127^-$, $KLRG1^+$, IL-$2^{+/-}$) (8, 11, 12) further underscores the influence of antigen-driven differentiation but costimulatory signals provided by TNFR family members such as CD27, OX40 and 4-1BB are required for inflation as well (13-15). In addition, CD4 T cell help facilitates the inflationary $CD8^+$ T cell response (16, 17). In contrast to exhausted T cells, which develop during infection with high-level replicating viruses (18), inflationary T cells remain functional throughout the lifetime of the host (5, 19-21), which provides prospects for the use of CMV-based vaccine vectors (1, 22-24).

The percentages of human CMV-specific T cells occupying the memory T cell compartment vary greatly among seropositive individuals (25, 26). Moreover, the effector memory phenotype of CMV-specific T cells varies among individuals and seems to correlate with the memory $CD8^+$ T cell pool size (26-29). In this respect, it is of interest to note that the viral dose which humans become infected with likely varies within a large range as bodily fluids such as breast milk, saliva and urine, causing horizontal transmission of CMV, contain different quantities of CMV among individuals ranging from 10^1 to 10^5 copies/µl (30, 31). Thus, it appears that the degree of memory T cell inflation differs per CMV-infected host but whether this is linked to the initial viral inoculum dose is unknown.

In this study, we examined the influence of the viral inoculum size on the course of CMV infection and on memory T cell inflation in particular by using an experimental model of CMV, i.e. mouse CMV, which mimics human CMV infection. We found that low dose viral inoculum in contrast to high dose resulted in severely hampered memory T cell inflation, which is accompanied by a more central memory phenotype of the inflationary T cells and improved capacity to expand after re-challenge. These findings are of importance for vaccination strategies against CMV and for the development of CMV-based vaccine vectors.

MATERIALS AND METHODS

Mice

Wild-type (WT) C57BL/6 and BALB/c mice were purchased from Charles River. Thy1.1 (CD90.1) mice (obtained from The Jackson Laboratory) on a C57BL/6 background were

bred in-house. All mice were maintained under specific pathogen free (SPF) conditions at the Central Animal Facility of Leiden University Medical Center (LUMC) and were 8-10 weeks old at the beginning of each experiment. All animal experiments were approved by the Animal Experiments Committee of the LUMC and performed according to the Dutch Experiments on Animals Act that serves the implementation of 'Guidelines on the protection of experimental animals' by the Council of Europe and the guide to animal experimentation set by the LUMC.

MCMV infection and determination of viral load

MCMV-Smith was obtained from the American Type Culture Collection (ATCC VR-194; Manassas, VA) and salivary gland stocks were prepared from infected BALB/c mice. Mice matched for gender and age were infected i.p. with different dosages of salivary gland derived MCMV-Smith ranging from 10^1 to 10^4 PFU. For determination of viral load, genomic DNA was isolated from snap frozen tissues or from hematopoietic and non-hematopoietic cell splenic populations that were sorted based on the expression of CD45 using a DNAeasy blood and tissue kit (Qiagen, Venlo, Netherlands). MCMV glycoprotein B (gB) was then assayed by quantitative PCR using an IQ5 real time PCR detection system (Bio-Rad, Hercules, CA) and IQ SYBR Green MasterMix reagent (Bio-Rad). Aliquots (100 ng) of DNA were used as templates for each reaction. MCMV gB was used to determine MCMV viral load and MCMV copy numbers were calculated using a standard curve generated with the K181 MCMV plasmid. Data are expressed as MCMV copy number per 100 ng genomic DNA and normalized to β-actin. The limit of detection was 400 genome copies/100 ng DNA. The primer sequences used for detection of gB were 5'-GAAGATCCGCATGTCCTTCAG-3' and 5'-AATCCGTCCAACATCTTGTCG-3'. Primers used for detecting β-actin were 5'-GATGTCACGCACGATTTCC-3' and 5'-GGGCTATGCTCTCCCTCAC-3'. Real-time PCR data was analyzed using the Bio-Rad IQ5 software.

MCMV-specific antibody detection

Blood samples were collected retro-orbitally from infected mice at day 8, 60 and 120 post-infection. After brief centrifugation, sera were transferred to new tubes and stored at −20°C. MCMV-specific serum IgG levels were measured by ELISA. In short, 96 well plates (Nunc Maxisorp) were coated overnight at 4°C with NIH-3T3 derived MCMV-Smith in bicarbonate buffer (pH 9.6). Plates were subsequently incubated for 1 h at 37°C with blocking buffer (PBS/5% milk powder). Sera were diluted 1:500 in PBS/1% milk powder and incubated in the blocked wells for 1 h at 37°C. HRP-conjugated IgG_1, IgG_{2b}, IgG_{2c}, IgG_3 antibodies (Southern Biotech, Birmingham, USA) were diluted 1:4000 in PBS/1% milk powder and incubated 1 h at 37°C. To develop the plates 100 µl of TMB (3,3',5,5'-Tetramethylbenzidine) (Sigma Aldrich) was added to each well and incubated for 15 minutes at room temperature, after which 100 µl stop solution (1M H_2SO_4) was

added. Plates were measured within 5 minutes after adding stop solution at 450 nm using a Microplate reader (Model 680, Bio-Rad).

Flow cytometry

Single cell suspensions were prepared from spleen and lymph nodes by mincing the tissue through a 70 μm cell strainer (BD Bioscience). For lymphocyte isolation from the bone marrow, the tibias and femurs were removed and flushed followed by filtering through a 70 μm cell strainer. Erythrocytes were lysed in a hypotonic ammonium chloride buffer. Before lungs and liver were removed, mice were perfused with PBS containing EDTA to remove all blood associated lymphocytes. Lymphocytes were isolated from the lungs and liver by collagenase (crude, type IA) (Sigma Aldrich) and DNAse I (Sigma Aldrich) treatment for 0.5 h followed by percoll (GE Healthcare, Uppsala) gradient. Tetramer staining and intracellular cytokine staining were used to determine the magnitude and characteristics of the MCMV-specific T cell responses as described elsewhere (32). Fluorochrome-conjugated antibodies specific for CD3, CD8, CD25, CD44, CD45.1, CD45.2, CD90.1, CD90.2, CD127 (IL-7Rα), IFN-γ, IL-2, KLRG1, NK1.1, TNF, Ki67 and Bcl-2 were purchased from BD Biosciences, Biolegend or eBioscience. Dead cells were excluded by positivity for 7AAD (Invitrogen). Cells were acquired using a BD LSR II flow cytometer, and data was analyzed using FlowJo software (TreeStar).

Tetramers and peptides

The following class I-restricted peptides were used: $M45_{985\text{-}993}$, $m139_{419\text{-}426}$, $M38_{316\text{-}323}$, and $IE3_{416\text{-}423}$ (described in (12, 33)). MHC class I tetramer complexes for M45 (D^b restricted), m139, M38 and IE3 (all K^b restricted) were produced as described elsewhere (34).

Re-challenge and adoptive transfers

To determine the effect of the inoculum size on protective immunity, mice were infected with 10^1 or 10^4 PFU MCMV-Smith and 60 days post-infection these mice were re-infected with 10^5 PFU MCMV-Smith. One day before and 5 days after re-challenge, blood was taken and the magnitude of the response was determined by tetramer staining. To determine the secondary expansion capacity of MCMV-specific T cells after adoptive transfer, Thy1.1 mice were infected with 10^1 PFU or with 10^4 PFU MCMV-Smith. At day 60 post-infection, splenic M45-, M38- and IE3-specific $CD8^+$ T cells were stained with MHC class I tetramers and purified by sorting using a BD FACSAria II flow cytometer. Next, 1×10^3 $M45^+$, 3×10^3 $M38^+$ or 3×10^3 $IE3^+$ $CD8^+$ T cells were transferred i.v. into naive Thy1.2 mice. The host mice were infected 3 h later with 10^4 PFU MCMV-Smith and at day 5 post-infection the absolute numbers of donor M45-, M38- and IE3-specific $CD8^+$ T cells were determined in the spleen by tetramer staining.

To compare the secondary expansion capacity of central memory MCMV-specific $CD8^+$ T cells induced in low and high dose infected mice, Thy1.1 mice were infected with 10^1

PFU or with 10^4 PFU MCMV-Smith. At day 60 post-infection, splenic $CD127^+KLRG1^-$ M38-specific $CD8^+$ T cells were purified by sorting using a BD FACSAria II flow cytometer. Next, 3×10^3 of the sorted cells were transferred i.v. into naive Thy1.2 mice. The host mice were infected 3 h later with 10^4 PFU MCMV-Smith and at day 5 post-infection the absolute numbers of donor M38-specific $CD8^+$ T cells were determined in the spleen by MHC class I tetramer staining.

Statistical analysis

Statistical significance was assessed by the Mann-Whitney test using GraphPad Prism software. P values < 0.05 were considered significant.

RESULTS

The degree of memory T cell inflation is determined by the size of the viral inoculum

To determine the effect of the inoculum dose on the inflation of MCMV-specific memory T cell populations, C57BL/6 mice were infected with either 10^1 PFU (low dose) or 10^4 PFU (high dose) of MCMV Smith strain. Accordingly, both in the acute and chronic phase of infection, viral load in tissues (liver, lungs and salivary glands) determined by quantitative real-time PCR (qPCR) was lower in mice infected with 10^1 PFU MCMV as compared to infection with 10^4 PFU (Fig. 1A). Furthermore, the number of activated NK cells, which play an important role in limiting acute CMV replication, correlated to the viral dose (Fig. 1B). The MCMV-specific IgG2c antibody titers were reduced in low dose infected mice at day 8 post-infection. Inflation of IgG2c levels, however, was observed in both low and high dose infected mice (Fig. 1C). Similar results were obtained with other antibody IgG isotypes, i.e. IgG1, IgG2b, and IgG3 (data not shown).

In the acute phase of infection, the absolute splenic numbers of the non-inflationary M45-specific $CD8^+$ T cells were ~5-fold reduced in mice receiving low dose inoculum, and $CD8^+$ T cell numbers specific for the inflationary epitopes m139, M38 and IE3 were ~2 fold reduced (Fig. 1D). After the peak of the acute response (day 8), the M45-specific $CD8^+$ T cell response underwent similar contraction in the low and high dose infected mice. Remarkably, although MCMV infection in C57BL/6 mice is usually characterized by accumulation of m139-, M38- and IE3-specific $CD8^+$ T cells during the chronic phase, inflation of these populations is either absent (m139- and M38-specific) or rigorously impaired (IE3-specific) when the inoculum size is lowered to 10^1 PFU (Fig. 1E). Analogous to the spleen, the degree of memory T cell inflation in the lungs was impaired after low dose inoculum as compared to high dose (Fig. 1F). Thus low dose inoculum of MCMV still results in a persistent infection, but in contrast to high dose inoculum such infection is not accompanied by overt memory T cell inflation.

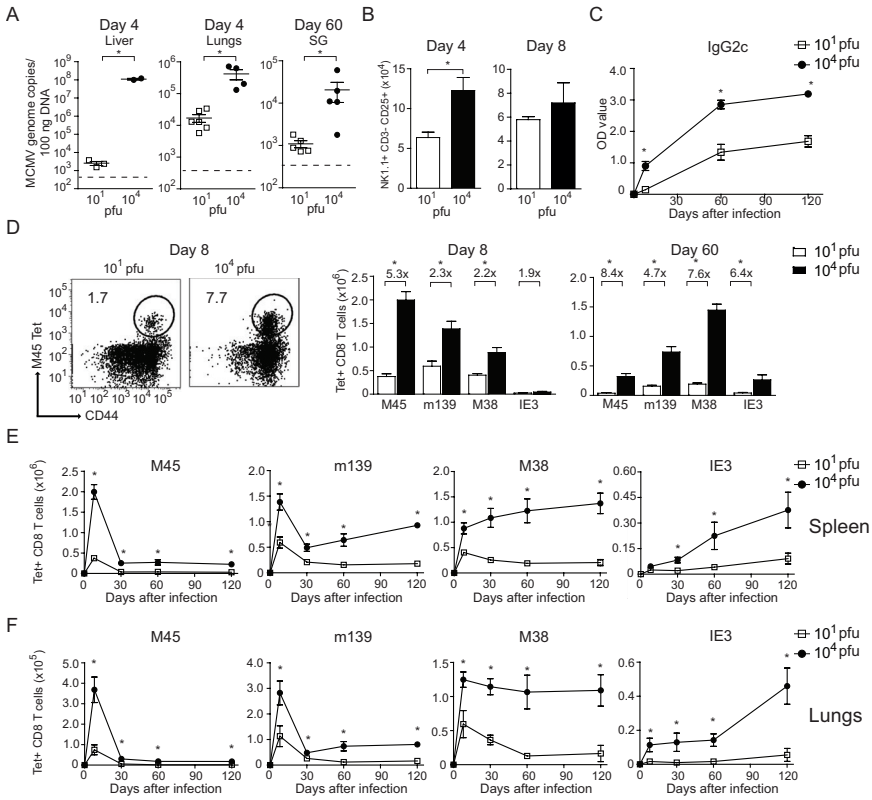

Figure 1. The degree of memory T cell inflation is determined by the size of the viral inoculum. WT mice were infected with 10^1 or 10^4 PFU MCMV-Smith. (A) Viral titers were determined in liver, lungs and salivary glands (SG) by quantitative real-time PCR at day 4 and 60 post-infection. Graphs depict MCMV genome copies per 100 ng tissue derived DNA. Each symbol represents an individual mouse. (B) Bar graphs depict the absolute number of splenic NK1.1$^+$/CD3$^-$ cells positively stained for CD25 at day 4 and 8 post-infection. (C) At day 8, 60 and 120 days post-infection serum samples were taken and MCMV specific IgG2c titers were determined by ELISA. Graph shows OD values measured at 450 nm. (D) At day 8 and 60 after infection, the magnitude of the CD8$^+$ T cell response to epitopes derived from the MCMV proteins M45, m139, M38 and IE3 was determined in the spleen using MHC class I tetramer staining. Representative flow cytometry plots show CD44 expression and binding to MHC class I M45 tetramers (Tet) on gated CD8$^+$ T cells at 8 day after infection. Bar graphs show the absolute number of splenic MCMV-specific CD8$^+$ T cells for each epitope at day 8 and 60 post-infection. (E and F) At day 8, 30, 60 and 120 after infection the magnitude of the CD8$^+$ T cell response to the indicated MCMV epitopes was examined in the spleen (E) and in the lungs (F). Graphs show the absolute number of MCMV-specific CD8$^+$ T cells for each epitope as determined by using MHC class I tetramers. Shown are mean values and SEM ($n = 4$). Statistical significance is determined by the Mann-Whitney test and indicated with an asterisk (* $p < 0.05$). Shown are representative data of three independent experiments.

Impaired memory T cell inflation during low dose infection relates to diminished latent virus in non-hematopoietic cells and to antigen-driven proliferation

Priming of CMV-specific T cells is thought to be dependent on cross-presenting hematopoietic antigen-presenting cells while memory T cell inflation, at least in the MCMV model, relies on infected non-hematopoietic cells (6, 10, 35). To evaluate whether the impaired memory T cell inflation after low dose inoculum relates to the amount and localization of (latent) MCMV, we aimed to quantify the presence of MCMV genomes by

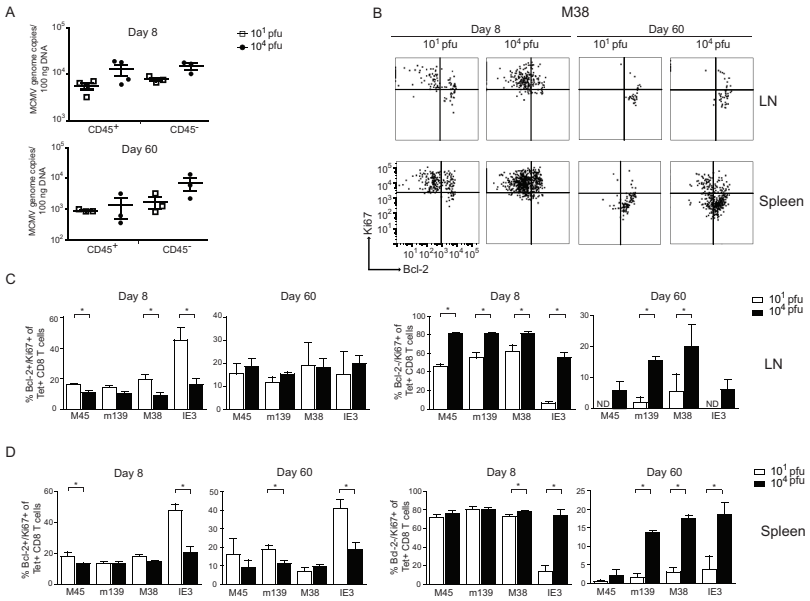

Figure 2. Reduced reservoirs of latent MCMV in non-hematopoietic cells and diminished antigen-driven T cell proliferation after low dose infection. WT mice were infected with 10^1 or 10^4 PFU MCMV-Smith. (A) Viral titers were determined in hematopoietic ($CD45^+$) and non-hematopoietic ($CD45^-$) spleen cells by quantitative real-time PCR at day 8 and 60 post-infection. Graphs depict MCMV genome copies per 100 ng DNA. Each symbol represents an individual mouse ($n = 3$). (B) Representative flow cytometry plots show expression of Bcl-2 and Ki67 on M38-tetramer$^+$ $CD8^+$ T cells derived from the spleen or LNs (axillary, brachial and inguinal) at day 8 and 60 after infection. (C) Bar graphs show the percentage of Bcl-2^+/Ki67^+ or Bcl-2^-/Ki67^+ expressing cells within the tetramer$^+$ $CD8^+$ T cell populations at day 8 and 60 post-infection in the LNs or (D) spleen. Shown are mean values and SEM ($n = 5$). Bcl-2^-/Ki67^+ M45- and IE3-specific T cells were not detectable (ND) in the lymph nodes at day 60 post-infection. Statistical significance is determined by the Mann-Whitney test and indicated with an asterisk (* $p < 0.05$). Shown are representative data of two independent experiments.

qPCR in hematopoietic ($CD45^+$) and non-hematopoietic ($CD45^-$) splenic cells during the acute and latent phase of infection. During the acute phase of infection, MCMV genomes were more abundantly present in both the hematopoietic and non-hematopoietic fraction of low and high dose inoculated mice while at day 60 post-infection, when memory T cell inflation occurs predominantly in high dose infected mice, MCMV localizes only in these mice at a higher level in the non-hematopoietic compartment (Fig. 2A). Thus besides affecting productive infection also the reservoir of latent MCMV genomes in non-hematopoietic cells is influenced by the initial viral dose. Consistent with previous findings (6, 10) this finding also suggests that latently infected non-hematopoietic cells are essential for driving memory T cell inflation.

To evaluate whether the reduced presence of MCMV genomes after low dose inoculum is related to impaired cycling activity of the inflationary memory T cells, we analyzed Ki-67 expression (associated with proliferation) together with the expression of the anti-apoptotic molecule Bcl-2 in order to discriminate between either antigen-driven proliferation (Bcl-2^-Ki-67^+) or cytokine-driven homeostatic proliferation (Bcl-2^+Ki-67^+). While

at day 8 post-infection, both in low and high dose infected mice the cycling activity of M45-, m139- and M38-specific CD8$^+$ T cells in spleen and lymph nodes was mainly antigen-driven, at late time-points post-infection the antigen-driven proliferation in these cells was still considerable in high dose infected mice but minute in low dose infected mice (Fig. 2B-D). Remarkably, IE3-specific CD8$^+$ T cells already show diminished antigen-driven proliferation at day 8 post-infection but show elevated cytokine-driven homeostatic proliferation at day 8 post-infection in spleen and lymph nodes and at day 60 in the spleen (Fig. 2B-D). Taken together, these results show that the impaired memory T cell inflation after low dose inoculum relates to reduced reservoirs of latent MCMV in non-hematopoietic cells and accordingly into diminished antigen-driven T cell proliferation.

Viral inoculum size influences central and effector memory CD8$^+$ T cell formation

Inflationary memory T cells are characterized by a predominant effector-like phenotype, whereas non-inflationary memory T cells have a principal central memory phenotype during the latent phase of infection (1). To evaluate whether the central/effector memory

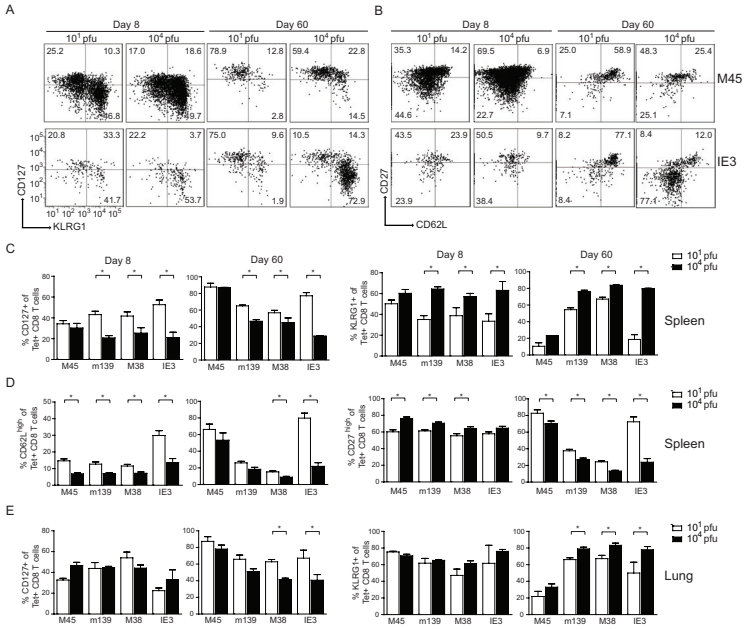

Figure 3. Viral inoculum size influences central and effector memory CD8$^+$ T cell formation. WT mice were infected with 10^1 or 10^4 PFU MCMV-Smith. (A) Representative flow cytometry plots show cell surface expression of CD127 and KLRG1 or (B) expression of CD27 and CD62L on splenic M45, m139, M38 and IE3 tetramer$^+$ CD8$^+$ T cells at day 8 and 60 after infection. (C and D) Bar graphs show the percentage of CD127, KLRG1, CD27 and CD62L expressing cells within the tetramer$^+$ CD8$^+$ T cell populations at day 8 and 60 post-infection in the spleen. (E) Bar graphs show the percentage of CD127 and KLRG1 expressing cells within the tetramer$^+$ CD8$^+$ T cell populations at day 8 and 60 post-infection in the lungs. Shown are mean values and SEM (n=4). Statistical significance is determined by the Mann-Whitney test and indicated with an asterisk (* $p < 0.05$). Shown are representative data of three independent experiments.

phenotype is related to the occurrence of inflation we examined the phenotype of MCMV-specific CD8$^+$ T cells after low and high dose viral inoculum. Regardless of the inoculum dose, the splenic M45-specific memory T cells cell surface markers associated with a central memory phenotype at day 60 post-infection (CD127$^+$KLRG1$^-$CD62L$^+$CD27^{high}) (Fig. 3A-D) while during acute infection (day 8), these cells display an effector-like phenotype (CD127$^-$KLRG1$^+$CD62L$^-$CD27^{low}). In contrast, the splenic m139- and M38-specific CD8$^+$ T cells display a reduced effector-like phenotype (CD127$^-$KLRG1$^+$CD62L$^-$CD27^{low}) in low dose infected animals during the acute and persistent phase of infection (Fig. 3A-D). Intriguingly, the CD8$^+$ T cells that react to the inflationary IE3 epitope have like the M45-specific CD8$^+$ T cells a predominant central memory phenotype (Fig. 3A-D). This shift in phenotype of the IE3-specific CD8$^+$ T cells in low dose infected mice is already clearly present in the acute phase of infection (day 8) and gradually becomes more pronounced. In the lungs, minimal differences in cell surface phenotype MCMV-specific CD8$^+$ T cells were observed between low and high dose infected during the acute phase of infection but at later time points the inflationary T cells were phenotypically less effector-like in low dose infected mice (Fig 3E).

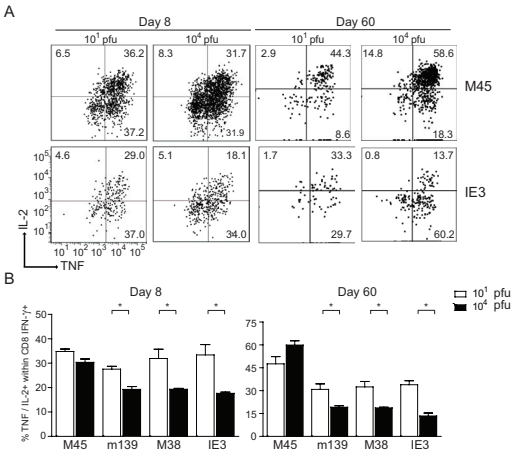

Figure 4. Inflationary MCMV-specific CD8$^+$ T cells in low dose infected hosts have increased IL-2 production. WT mice were infected with 10^1 or 10^4 PFU MCMV-Smith. (A) Representative flow cytometry plots show intracellular TNF and IL-2 production within the splenic IFN-γ^+ CD8$^+$ T cells after restimulation with M45 or IE3 class I peptides at day 8 and 60 post-infection. (B) Bar graphs show the percentages of TNF$^+$ IL-2$^+$ cells within splenic IFN-γ^+ CD8$^+$ T cell populations after restimulation with the indicated peptides at day 8 and 60 post-infection. Shown are mean values and SEM (n=4). Statistical significance is determined by the Mann-Whitney test and indicated with an asterisk (* $p < 0.05$). Shown are representative data of three independent experiments.

As observed with the analysis of the phenotypic cell-surface markers, the percentage of IL-2$^+$TNF$^+$ but not the IL-2$^-$TNF$^+$ expressing cells within the inflationary m139-, M38- and IE3-specific CD8$^+$ T cell pools was increased in low dose infected hosts, which also points to a more central memory phenotype (Fig. 4A and B). The IL-2 production by the non-inflationary M45-specific CD8$^+$ T cells was unaltered by varying the viral inoculum size. When intermediate inoculum sizes of 10^2 and 10^3 PFU were used to infect mice also intermediate phenotypes and degrees of memory inflation were observed (data not shown). Together, these results indicate that the phenotype of inflationary MCMV-specific CD8$^+$ T cells is influenced by the viral dose. In addition, the data instill that already early after infection phenotypic analysis of inflationary T cells can be used to predict the occurrence of inflation during the persistent phase of infection.

Organ distribution of IE3-specific CD8⁺ T cells correlates with the shift towards central memory phenotype in low dose infection

Central memory and effector memory T cells are characterized not only by their difference in effector function but also by their distinct homing capacity (36). While central memory T cells preferentially home to lymphoid organs, effector memory T cells have the capacity to migrate throughout the whole body. To address whether the skewing towards a more central memory-like phenotype in low dose infection resulted in alterations in tissue distribution of MCMV-specific CD8⁺ T cells, mice were infected with 10^1 or 10^4 PFU MCMV and absolute numbers of MCMV-specific CD8⁺ T cells were determined in lymphoid (inguinal lymph nodes (ILN), and bone marrow) and non-lymphoid tissues (lungs, and liver) at day 30 post-infection. In all these tissues the absolute numbers of MCMV-specific CD8⁺ T cells were as anticipated lesser in low dose infected mice (Fig. 5A and B). The organ distribution of M45-specific CD8⁺ T cells is not different between infection with 10^1 and 10^4 PFU MCMV, which is in accordance with the observation that M45-specific T cells display a central memory phenotype independently of the size of the viral inoculum. Despite the moderate differences in phenotype, the m139- and M38-specific CD8⁺ T cell populations exhibited minute differences in organ distribution when comparing the low and high inoculum sizes. During the course of low

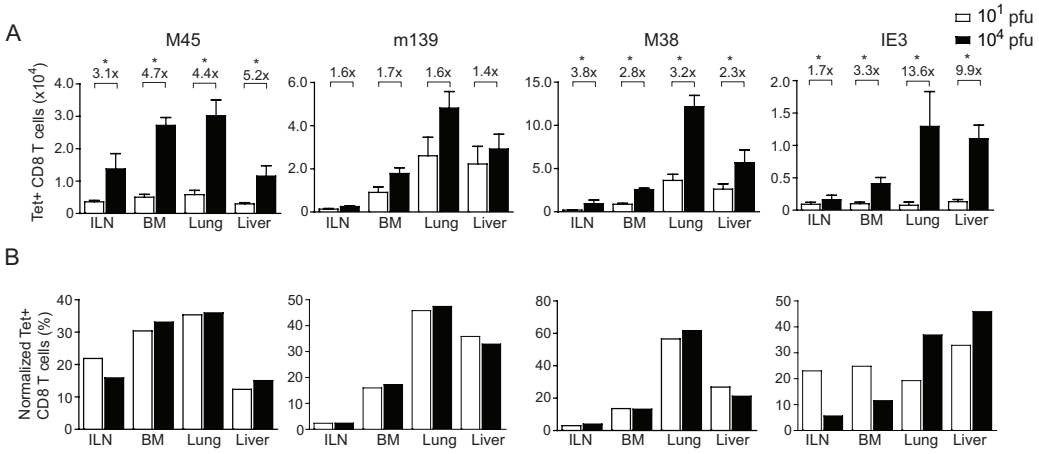

Figure 5. Organ distribution of IE3-specific CD8⁺ T cells correlates with a strong shift towards central memory phenotype in low dose infection. WT mice were infected with 10^1 or 10^4 PFU MCMV-Smith and at day 30 after infection the CD8⁺ T cell response to the indicated MCMV epitopes was examined in inguinal lymph nodes (ILN), bone marrow, lungs and liver. (A) Depicted are absolute numbers of M45-, m139-, M38- and IE3-specific CD8⁺ T cells as measured by MHC class I tetramer binding. (B) For each tetramer separately, the absolute numbers of tetramer⁺ CD8⁺ T cells per tissue were normalized to the total count of the tetramer⁺ CD8⁺ T cells in ILN, bone marrow, lungs and liver. Bar graphs show mean and SEM (n=4 per experiment). Statistical significance is determined by the Mann-Whitney test and indicated with an asterisk (* $p < 0.05$). Shown are pooled data of two independent experiments.

dose infection the IE3-specific CD8$^+$ T cells preferentially migrated to the ILN and bone marrow but homed lesser to the lungs and liver compared to high dose inoculum (Fig. 5A and B). Together, these data infer that the migratory properties of IE3-specific CD8$^+$ T cells are influenced by the initial viral dose, which is consistent with the strong shift of these cells towards a central memory phenotype.

Improved secondary expansion capacity of inflationary memory CD8$^+$ T cells elicited during low dose infection

Immunological memory is the ability of the immune system to respond faster and more effective upon secondary challenge with the same antigen and constitutes the basis for vaccination. To examine the effects of the inoculum size on protective immunity and secondary responses, mice were infected with 10^1 or 10^4 PFU MCMV and after 60 days the same mice were re-challenged using 10^5 PFU MCMV (Fig. 6A). The viral loads in the low and high dose infected mice were comparable after re-challenge and significantly lower as compared to mice that were not exposed to MCMV prior to the challenge, indicating that low dose inoculation protects as well as high dose (Fig. 6B). The secondary expansion potential of the inflationary m139-, M38- and IE3-specific but not of the non-inflationary M45-specific memory CD8$^+$ T cells was improved after low dose infection compared to high dose infection (Fig. 6C). However, certain conditions such as T cell competition and differences in innate and humoral immunity between low and high dose challenged mice could influence the T cell expansion rate. To create conditions in which the secondary expansion capacity of the MCMV specific CD8$^+$ T cells could be examined without such confounding factors, we adoptively transferred congenically marked (Thy1.1) non-inflationary (M45-specific) or inflationary (M38 and IE3-specific) memory CD8$^+$ T cells from low and high dose infected mice into naive (Thy1.2) recipients and subsequently challenged these recipients with MCMV (Fig. 6D). No difference was observed between the secondary expansion capacity of M45-specific CD8$^+$ T cells that originated from mice infected with either low or high dose PFU whereas M38 and IE3-specific T cells of low dose infected mice expanded better compared to M38 and IE3-specific CD8$^+$ T cells from high dose infected mice (Fig. 6E). Our observation that M45-specific T cells respond better than inflationary cells after adoptive transfer in naive mice, while in re-challenged mice that contain high numbers of inflationary T cells the expansion of M45-specific T cells is relatively reduced as compared to the inflationary T cells might be explained by competition among MCMV- specific T cell pools as has been described recently (37, 38).

As central memory T cells are known to have a better expansion potential as compared to effector memory T cells (39, 40), our findings are consistent with the raised central memory phenotype of the inflationary T cells in low dose infected mice. To determine whether there are differences among inflationary T cells with a central memory-like phenotype elicited either in a low or high dose infection, we sorted congenically marked

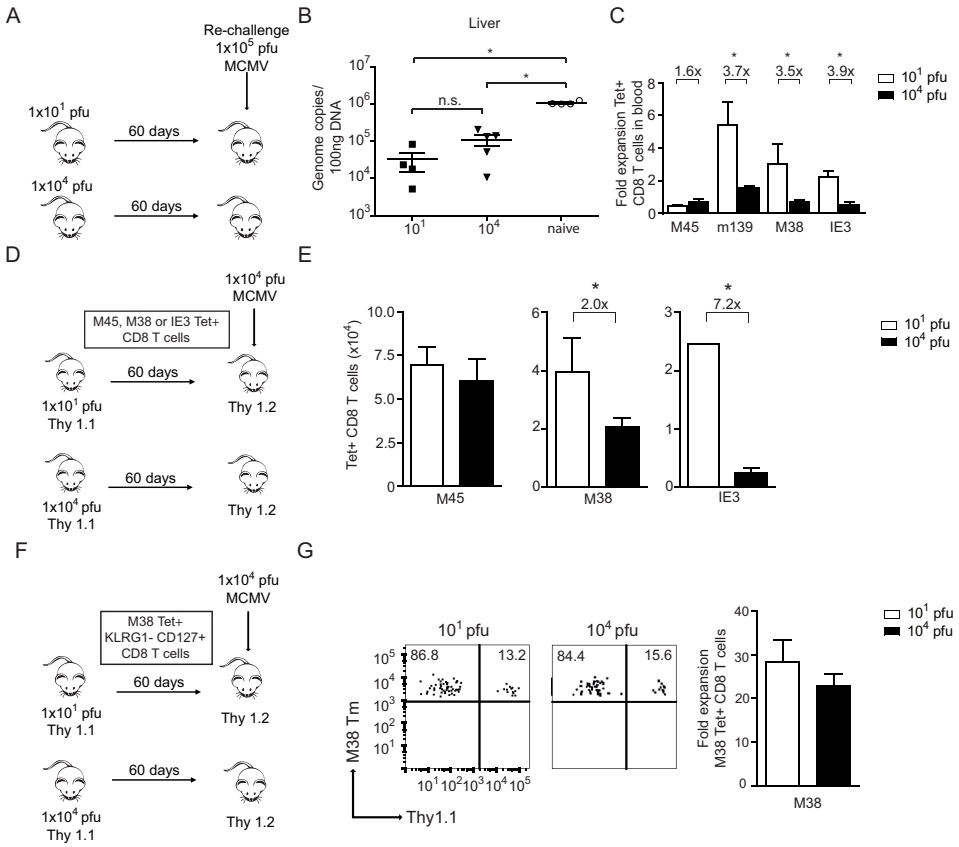

Figure 6. Improved secondary expansion capacity of MCMV-specific CD8⁺ T cells induced by low viral dose. (A) Schematic of the experimental setup. WT mice were infected with 10^1 or 10^4 PFU MCMV-Smith and 60 days after infection the same mice were re-challenged with 10^5 PFU MCMV-Smith. At the same time naive mice also received a challenge with 10^5 PFU MCMV-Smith. (B) Graphs indicate the number of MCMV copies per 100 ng liver derived DNA at day 5 post re-challenge. Each symbol represents an individual mouse. (C) One day before and 5 days after re-challenge the CD8⁺ T cell response to the indicated MCMV epitopes was determined by MHC class I tetramer staining in blood. Bar graph shows fold expansion of the MCMV-specific CD8⁺ T cell response after re-challenge. (D) Schematic of the experimental setup. Thy1.1 mice were infected with 10^1 or with 10^4 PFU MCMV-Smith. After 60 days M45, M38 and IE3 tetramer⁺ CD8⁺ T cells were sorted and transferred into naive Thy1.2 recipients, which were subsequently infected with 10^4 PFU MCMV-Smith. (E) Bar graphs show the absolute number of MCMV-specific CD8⁺ T cells in the spleen at day 5 post-infection. (F) Schematic of the experimental setup. Thy1.1 mice were infected with 10^1 or 10^4 PFU MCMV-Smith. After 60 days CD127⁺KLRG1⁻ M38-specific CD8⁺ T cells were sorted and transferred into naive Thy1.2 recipients, which were subsequently infected with 10^4 PFU MCMV-Smith. (G) Representative flow cytometry plots show cell surface expression of Thy1.1 (CD90.1) on splenic M38 tetramer⁺ CD8⁺ T cells at day 5 post-infection. Bar graph shows fold expansion of the MCMV-specific central memory CD8⁺ T cells in the spleen. Bar graph data show mean values and SEM (n=4). Statistical significance is determined by the Mann-Whitney test and indicated with an asterisk (* $p < 0.05$). Shown are representative data of two independent experiments.

(Thy1.1) central memory-like (CD127⁺KLRG1⁻) M38-specific T cells from low and high dose infected mice and adoptively transferred equal numbers of these cells in naive mice (Thy1.2 cells). After challenge, we observed a similar expansion capacity indicating that no intrinsic difference among central memory-like inflationary T cells occurs after a low or high dose inoculum. Thus, low dose viral inoculum elicits inflationary memory CD8⁺

T cells with an improved secondary expansion capacity on a population level consistent with a central memory phenotype.

DISCUSSION

In this study we show that the degree of memory T cell inflation is directly influenced by the size of the viral inoculum. This report also highlights the impact of the inoculum dose on the ratio of effector memory versus central memory phenotype within an antigen-specific T cell population; a low viral inoculum size skews the "inflationary" $CD8^+$ T cells, or to be more specific the $CD8^+$ T cells with the ability to undergo memory inflation, towards a central memory phenotype ($CD127^+$, $KLRG1^-$, $CD27^{high}$, $CD62L^+$, $IL\text{-}2^+$), whereas in high dose infection these T cells are more effector memory like ($CD127^-$, $KLRG1^+$, $CD27^{low}$, $CD62L^-$, $IL\text{-}2^{+/-}$). These data provide reasoning for the dissimilarity in terms of magnitude and phenotype of CMV-specific T cell responses as observed in human CMV-infected individuals (25-29).

Inflationary T cell responses are elicited by both immediate early (IE) (e.g. IE3 in C57BL/6 mice and IE1 in BALB/c mice) and early (E) antigens (e.g. m139 and M38 in C57BL/6 mice and m164 in BALB/c mice), albeit with different kinetics and magnitude (12, 41). We observed that the memory phenotype of the IE3-specific T cells was mostly affected by the viral inoculum size as compared to the m139- and M38-specific T cells. Nevertheless, strongly impaired but still detectable memory T cell inflation was detected against IE3 whereas no inflation was observed against m139 and M38 in low dose infected mice. These apparent differences between T cell responses against IE and E antigens point to different mechanisms how these antigens can provoke memory T cell inflation. Reddehase and colleagues have shown that transcriptional reactivation occurs for IE antigens in the lungs and liver (7, 42), and may drive memory inflation (42). Such transcriptional reactivation in non-lymphoid tissues is not found or at least to a lesser extend for E antigens, which could be related to a lower incidence or weaker promoter activity (43). Recent data by Oxenius and colleagues indicated that for memory inflation of M38-specific T cells, the lymphoid organs are instead important (10). Whether transcriptional reactivation is important to inflate memory T cells in the lymphoid organs is undetermined. Besides potential differences in antigenic triggering of IE and E antigen-specific T cells, these cells may also differentially depend on (inflammatory) cytokines and costimulation. If indeed different mechanisms exist for memory T cell inflation specific for the M38 (and m139) versus IE3 antigens, it may explain some of our findings. Such differences might surface more prominently when limited antigen or alternatively less inflammatory/costimulatory signals are available to sustain MCMV-specific T cell populations. It is thought that the generation and sustainment of high levels of effector-memory T cells induced by CMV-based vaccine vectors is important for protective immunity

against the targeted pathogens (22-24). Based on our results, this suggests that high dose inoculums are important for the success of such CMV-based vaccines. Conversely, in case of protection against CMV itself it seems that low dose infection is equally capable to induce protective immunity as compared to high dose infection. Nevertheless, neither low nor high dose inoculum is able to induce sterile immunity but whether sterile immunity against CMV is possible at all given the numerous immune evasion mechanisms of CMV (44, 45) remains an open question. Thus far it was found that the immune components that are involved in protective immunity against CMV re-infection/activation point to a role of antibodies and $CD8^+$ T cells (7, 46-51), but many particulars still need to be addressed. In this respect, it is also interesting to note that during primary acute infection NK cells and $CD4^+$ T cells but not antibodies and $CD8^+$ T cells are critically involved in controlling viral replication.

Related to the subject of protective immunity and vaccination is conceivably the importance of the balance between effector and central memory T cells. Depending on the features of the pathogen, either central memory or effector memory T cells constitute superior protection compared to the other (39, 40). The apparent influence of the viral inoculum size on the balance between central memory and effector memory $CD8^+$ T cells within the "inflationary" $CD8^+$ T cell pools upon MCMV infection might be exploited for future vaccine development.

ACKNOWLEDGEMENTS

We would like to thank Kees Franken and Edwin de Haas for technical assistance. This work was supported by a Gisela Thier grant from Leiden University Medical Center to R.A.

REFERENCE LIST

1. O'Hara, G.A., et al., Memory T cell inflation: understanding cause and effect. *Trends Immunol*. 2012; 33: 84-90.
2. Holtappels, R., et al., Enrichment of immediate-early 1 (m123/pp89) peptide-specific CD8 T cells in a pulmonary CD62L(lo) memory-effector cell pool during latent murine cytomegalovirus infection of the lungs. *J. Virol*. 2000; 74: 11495-11503.
3. Komatsu, H., et al., Population analysis of antiviral T cell responses using MHC class I-peptide tetramers. *Clin. Exp. Immunol*. 2003; 134: 9-12.
4. Karrer, U., et al., Memory inflation: continuous accumulation of antiviral CD8+ T cells over time. *J. Immunol*. 2003; 170: 2022-2029.
5. Cicin-Sain, L., et al., Cytomegalovirus-specific T cell immunity is maintained in immunosenescent rhesus macaques. *J. Immunol*. 2011; 187: 1722-1732.
6. Seckert, C.K., et al., Antigen-presenting cells of haematopoietic origin prime cytomegalovirus-specific CD8 T-cells but are not sufficient for driving memory inflation during viral latency. *J. Gen. Virol*. 2011; 92: 1994-2005.

7. Simon, C.O., et al., CD8 T cells control cytomegalovirus latency by epitope-specific sensing of transcriptional reactivation. *J. Virol*. 2006; 80: 10436-10456.
8. Snyder, C.M., et al., Memory inflation during chronic viral infection is maintained by continuous production of short-lived, functional T cells. *Immunity*. 2008; 29: 650-659.
9. Snyder, C.M., et al., Sustained CD8+ T cell memory inflation after infection with a single-cycle cytomegalovirus. *PLoS. Pathog*. 2011; 7: e1002295.
10. Torti, N., et al., Non-hematopoietic cells in lymph nodes drive memory CD8 T cell inflation during murine cytomegalovirus infection. *PLoS. Pathog*. 2011; 7: e1002313.
11. Sierro, S., R. Rothkopf, and P. Klenerman, Evolution of diverse antiviral CD8+ T cell populations after murine cytomegalovirus infection. *Eur. J. Immunol*. 2005; 35: 1113-1123.
12. Munks, M.W., et al., Four distinct patterns of memory CD8 T cell responses to chronic murine cytomegalovirus infection. *J. Immunol*. 2006; 177: 450-458.
13. Welten, S.P., et al., CD27-CD70 costimulation controls T cell immunity during acute and persistent cytomegalovirus infection. *J. Virol*. 2013; 87: 6851-6865.
14. Humphreys, I.R., et al., OX40 costimulation promotes persistence of cytomegalovirus-specific CD8 T Cells: A CD4-dependent mechanism. *J. Immunol*. 2007; 179: 2195-2202.
15. Humphreys, I.R., et al., Biphasic role of 4-1BB in the regulation of mouse cytomegalovirus-specific CD8(+) T cells. *Eur. J. Immunol*. 2010; 40: 2762-2768.
16. Snyder, C.M., et al., CD4+ T cell help has an epitope-dependent impact on CD8+ T cell memory inflation during murine cytomegalovirus infection. *J. Immunol*. 2009; 183: 3932-3941.
17. Walton, S.M., et al., T-cell help permits memory CD8(+) T-cell inflation during cytomegalovirus latency. *Eur. J. Immunol*. 2011; 41: 2248-2259.
18. Wherry, E.J. and R. Ahmed, Memory CD8 T-cell differentiation during viral infection. *J. Virol*. 2004; 78: 5535-5545.
19. Komatsu, H., et al., Large scale analysis of pediatric antiviral CD8+ T cell populations reveals sustained, functional and mature responses. *Immun. Ageing*. 2006; 3: 11.
20. Wallace, D.L., et al., Human cytomegalovirus-specific CD8(+) T-cell expansions contain long-lived cells that retain functional capacity in both young and elderly subjects. *Immunology*. 2011; 132: 27-38.
21. Lelic, A., et al., The polyfunctionality of human memory CD8+ T cells elicited by acute and chronic virus infections is not influenced by age. *PLoS. Pathog*. 2012; 8: e1003076.
22. Hansen, S.G., et al., Profound early control of highly pathogenic SIV by an effector memory T-cell vaccine. *Nature*. 2011; 473: 523-527.
23. Tsuda, Y., et al., A replicating cytomegalovirus-based vaccine encoding a single Ebola virus nucleoprotein CTL epitope confers protection against Ebola virus. *PLoS. Negl. Trop. Dis*. 2011; 5: e1275.
24. Karrer, U., et al., Expansion of protective CD8+ T-cell responses driven by recombinant cytomegaloviruses. *J. Virol*. 2004; 78: 2255-2264.
25. Sylwester, A.W., et al., Broadly targeted human cytomegalovirus-specific CD4+ and CD8+ T cells dominate the memory compartments of exposed subjects. *J. Exp. Med*. 2005; 202: 673-685.
26. Lachmann, R., et al., Polyfunctional T cells accumulate in large human cytomegalovirus-specific T cell responses. *J. Virol*. 2012; 86: 1001-1009.
27. Gamadia, L.E., et al., Differentiation of cytomegalovirus-specific CD8(+) T cells in healthy and immunosuppressed virus carriers. *Blood*. 2001; 98: 754-761.
28. Gamadia, L.E., et al., The size and phenotype of virus-specific T cell populations is determined by repetitive antigenic stimulation and environmental cytokines. *J. Immunol*. 2004; 172: 6107-6114.
29. Iancu, E.M., et al., Clonotype selection and composition of human CD8 T cells specific for persistent herpes viruses varies with differentiation but is stable over time. *J. Immunol*. 2009; 183: 319-331.
30. Cope, A.V., et al., Quantity of cytomegalovirus viruria is a major risk factor for cytomegalovirus disease after renal transplantation. *J. Med. Virol*. 1997; 52: 200-205.
31. Kouri, V., et al., Diagnosis and screening for cytomegalovirus infection in pregnant women in Cuba

as prognostic markers of congenital infection in newborns: 2007-2008. *Pediatr. Infect. Dis. J*. 2010; 29: 1105-1110.

32. Arens, R., et al., Differential B7-CD28 costimulatory requirements for stable and inflationary mouse cytomegalovirus-specific memory CD8 T cell populations. *J. Immunol*. 2011; 186: 3874-3881.
33. Munks, M.W., et al., Genome-wide analysis reveals a highly diverse CD8 T cell response to murine cytomegalovirus. *J. Immunol*. 2006; 176: 3760-3766.
34. Altman, J.D., et al., Phenotypic analysis of antigen-specific T lymphocytes. *Science*. 1996; 274: 94-96.
35. Busche, A., et al., Priming of CD8+ T cells against cytomegalovirus-encoded antigens is dominated by cross-presentation. *J. Immunol*. 2013; 190: 2767-2777.
36. Sallusto, F., J. Geginat, and A. Lanzavecchia, Central memory and effector memory T cell subsets: function, generation, and maintenance. *Annu. Rev. Immunol*. 2004; 22: 745-763.
37. Farrington, L.A., et al., Competition for antigen at the level of the APC is a major determinant of immunodominance during memory inflation in murine cytomegalovirus infection. *J Immunol*. 2013; 190: 3410-6.
38. Dekhtiarenko, I., et al., The context of gene expression defines the immunodominance hierarchy of cytomegalovirus antigens. *J. Immunol*. 2013; 190: 3399-3409.
39. Bachmann, M.F., et al., Functional properties and lineage relationship of CD8+ T cell subsets identified by expression of IL-7 receptor alpha and CD62L. *J. Immunol*. 2005; 175: 4686-4696.
40. Wherry, E.J., et al., Lineage relationship and protective immunity of memory CD8 T cell subsets. *Nat. Immunol*. 2003; 4: 225-234.
41. Holtappels, R., et al., Two antigenic peptides from genes m123 and m164 of murine cytomegalovirus quantitatively dominate CD8 T-cell memory in the H-2d haplotype. *J. Virol*. 2002; 76: 151-164.
42. Seckert, C.K., et al., Liver sinusoidal endothelial cells are a site of murine cytomegalovirus latency and reactivation. *J. Virol*. 2009; 83: 8869-8884.
43. Seckert, C.K., et al., Viral latency drives 'memory inflation': a unifying hypothesis linking two hallmarks of cytomegalovirus infection. *Med Microbiol Immunol*. 2012; 201: 551-66.
44. Mocarski, E.S., Jr., Immunomodulation by cytomegaloviruses: manipulative strategies beyond evasion. *Trends Microbiol*. 2002; 10: 332-339.
45. Arens, R., Rational design of vaccines: learning from immune evasion mechanisms of persistent viruses and tumors. *Adv. Immunol*. 2012; 114: 217-243.
46. Jonjic, S., et al., Antibodies are not essential for the resolution of primary cytomegalovirus infection but limit dissemination of recurrent virus. *J. Exp. Med*. 1994; 179: 1713-1717.
47. Nigro, G., et al., Passive immunization during pregnancy for congenital cytomegalovirus infection. *N. Engl. J. Med*. 2005; 353: 1350-1362.
48. Klenovsek, K., et al., Protection from CMV infection in immunodeficient hosts by adoptive transfer of memory B cells. *Blood*. 2007; 110: 3472-3479.
49. Wirtz, N., et al., Polyclonal cytomegalovirus-specific antibodies not only prevent virus dissemination from the portal of entry but also inhibit focal virus spread within target tissues. *Med. Microbiol. Immunol*. 2008; 197: 151-158.
50. Walter, E.A., et al., Reconstitution of cellular immunity against cytomegalovirus in recipients of allogeneic bone marrow by transfer of T-cell clones from the donor. *N. Engl. J. Med*. 1995; 333: 1038-1044.
51. Reddehase, M.J., et al., Interstitial murine cytomegalovirus pneumonia after irradiation: characterization of cells that limit viral replication during established infection of the lungs. *J. Virol*. 1985; 55: 264-273.